Biochemical and Biophysical Research Communications 436 (2013) 719–724

Contents lists available at SciVerse ScienceDirect

Biochemical and Biophysical Research Communications

journal homepage: www.elsevier.com/locate/ybbrc

An attenuating role of a WASP-related protein, WASP-B, in the regulation of F-actin polymerization and pseudopod formation via the regulation of RacC during *Dictyostelium* chemotaxis

Chang Y. Chung [a,b,*], Alexander Feoktistov [b], Ryan J. Hollingsworth [a], Francisco Rivero [c], Nicole S. Mandel [b]

[a] Department of Pharmacology, Vanderbilt University Medical Center, Nashville, TN, USA
[b] Department of Biological Sciences, School of Art and Sciences, Vanderbilt University, Nashville, TN, USA
[c] Clinical Biosciences Institute, University of Hull, Hull, UK

ARTICLE INFO

Article history:
Received 31 May 2013
Available online 17 June 2013

Keywords:
Chemotaxis
WASP
F-actin
Dictyostelium

ABSTRACT

The WASP family of proteins has emerged as important regulators that connect multiple signaling pathways to regulate the actin cytoskeleton. *Dictyostelium* cells express WASP, as well as a WASP related protein, WASP-B, endoded by *wasB* gene. WASP-B contains many of the domains present in WASP. Analysis of wild type, *wasB* null cells revealed that WASP-B is required for proper control of F-actin polymerization in response to a cAMP gradient. Due to the lack of tight control on actin polymerization, *wasB* null cells exhibited higher level of F-actin polymerization. *wasB*$^-$ cells extend more *de novo* pseudopods laterally and their average life span is longer than those of wild type cells, causing more turns and inefficient chemotaxis. YFP-WASP-B appears to be uniformly distributed in the cytosol and shows no translocation to cortical membrane upon cAMP stimulation. Active RacC pull-down assay reveals that the level of active RacC in *wasB*$^-$ cells is significantly higher than wild type cells. Moreover, the distribution of active RacC is not localized in *wasB*$^-$ cells. We conclude that chemotaxis defects of *wasB*$^-$ cells are likely to result from the aberrant regulation of RacC activation and localization.

1. Introduction

Chemotaxis, a directed migration of cells, is a critical component of many biological processes. Cell migration is fueled by the reorganization of the actin cytoskeleton, thus it is essential to explore and comprehend the signaling pathways that regulate dynamics of F-actin organization. The WASP family of proteins, including WASP, N-WASP, and SCAR or WAVE, has emerged as important regulators that connect multiple signaling pathways to regulate the actin cytoskeleton in response to a chemoattractant [1,2]. WASP is held in an inactive state by an auto-inhibitory domain, which is relieved upon binding of activated Rac/Cdc42 and phospholipids, such as PI(4,5)P_2 or PI(3,4,5)P_3 [3,4]. WASP's C-terminal A segment has been shown to activate the Arp2/3 complex, a crucial component necessary to nucleate actin filaments [5,6]. Two of the seven subunits of the Arp2/3 complex, Arp2 and 3 are structurally similar to monomeric actin, which allows them to serve as nucleation sites for new actin filaments [7]. The Arp2/3 complex binds to the sides or the barbed end of existing filaments and initiates the growth of a new filament at a 70° angle, creating an expansive network of branching actin fibers [8,9].

The social amoeba *Dictyostelium Discoideum* utilizes similar mechanisms as mammalian systems to regulate chemotaxis. A *Dictyostelium* homologue of WASP was discovered and studies of WASP mutants in *Dictyostelium* have revealed WASP's critical role in cell polarization and localization of F-actin in response to a chemoattractant [10]. *Dictyostelium* genome has a gene (*wasB*; sequence ID: DDB0232169) encoding a WASP-related protein, WASP-B, with a significant sequence homology to WASP [11,12]. In this study, we examined the role of WASP-B, in the regulation of F-actin organization and chemotaxis of *Dictyostelium*. Analysis of *wasB* null *Dictyostelium* cells revealed that WASP-B is required for proper F-actin polymerization and chemotaxis in response to a cAMP gradient. *wasB* null cells exhibited a higher level of F-actin polymerization for a sustained period of time upon cAMP stimulation and extend more pseudopods with longer life span than those of wild type cells, causing more turns and inefficient chemotaxis. From these results, we conclude that WASP-B plays an attenuating role in the regulation of F-actin polymerization that is important for the regulation of the dynamics of pseupod extension and retraction.

* Corresponding author. Address: 468 Robinson Research Building (MRB I), 1215 21st Ave., South @ Pierce, Nashville, TN 37232-6600, USA. Fax: +1 615 343 6532.
E-mail address: chang.chung@vanderbilt.edu (C.Y. Chung).

0006-291X/$ - see front matter © 2013 Elsevier Inc. All rights reserved.
http://dx.doi.org/10.1016/j.bbrc.2013.06.022

2. Materials and methods

2.1. Cell culture and molecular biology

D. discoideum cells were cultured in HL5 medium supplemented with 60 U of penicillin and 60 μg of streptomycin per ml. The plasmid for homologous recombination was constructed by insertion of Bsr gene cassette into the *wasB* ORF at the *Sty*I site. YFP-WASP-B expression construct was produced by PCR amplification of *wasB* from cDNA library and subcloned into the pEXP4(+) vector in frame with eYFP at the N-terminus separated by the flexible linker GSGSG. Yeast two-hybrid assays were performed as described previously [13].

In vivo and *in vitro* actin polymerization assays were performed as described [10].

2.2. Chemotaxis assay

Chemotaxis assays were done as previously described [14]. Cells competent to chemotaxis toward cAMP (aggregation-competent cells) were plated on glass-bottomed microwell dishes (MarTek, Inc., Ashland, MA). A micropipette filled with 100 μM cAMP was positioned to stimulate cells by using a micromanipulator (Eppendorf), and the response and movement of cells were recorded by using Metamorph software (1 image per every 6 s). Cell movement was examined by tracing the movement of a single cell in a stack of images.

2.3. Active RacC pull-down assay

A×3 and *wasB*$^-$ cells expressing CFP-RacC were pulsed with 50 nM cAMP at 6-min intervals for 5 h. Cells were then shaken at 200 rpm with 3 mM caffeine for 20 min, washed twice, and resuspended in 2 mL Na/K buffer. 100 μl of cells were lysed at 0, 10, 20, 30, 45, 60, and 80-s after global cAMP stimulation with 1 ml of the lysis buffer. Nuclei were removed by centrifugation at 2500*g* and GST-WBD (WH1, B, and GBD domains of WASP)-bound-agarose beads (4 μg in 150 μl) were added to the lysate. After an hour of incubation, beads were washed three times with TBS-tween and active RacC bound to GST-WBD beads were eluted with SDS–PAGE sample buffer and run on a 10% gel. Relative amount of active RacC was assessed by western blot assays.

3. Results and discussion

A BLAST search of the *Dictyostelium* genome reveals a WASP-related protein, WASP-B (wasB; sequence ID: DDB0232169) with a significant sequence homology to WASP [12]. wasB encodes a WASP-related protein, WASP-B, that shares functional domains with WASP (Fig. 1A), specifically the actin/Arp2/3-binding VCA region, the Cdc42/Rac-binding GBD domain, and the SH3-binding poly-proline domain. WASP-B lacks the N-terminal WH1 and the basic domains of WASP. To examine the role of WASP-B, *wasB* null cells were created by homologous recombination, which was confirmed by Southern blot (Fig. 1B).

3.1. Loss of F-actin organization polarity in wasB$^-$ cells

We examined F-actin organization of wild type A×3 and *wasB*$^-$ cells by rhodamine-phalloidin staining (Fig. 1C). In aggregation-competent A×3 cells, F-actin organization is highly polarized with F-actin localized at the anterior leading edge and, to a lesser degree, the posterior of the cell [15]. Fluorescence intensity measured along the longitudinal axis was significantly greater than the intensity along the lateral axis in aggregation-competent wild type A×3

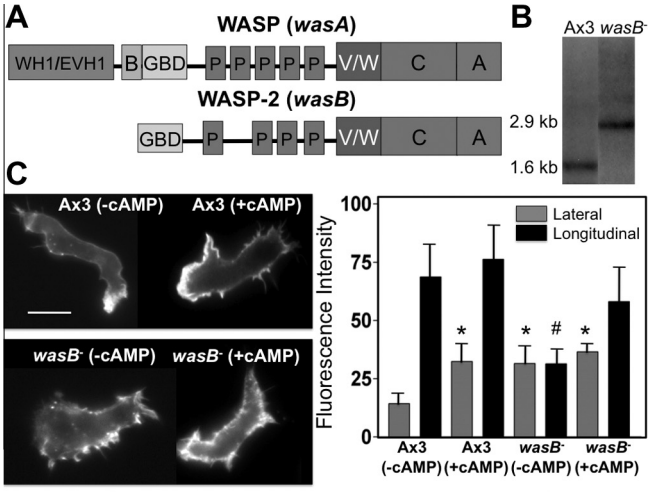

D

Rho GTPase	Interaction	
	WASP	WASP-B
Rac1b G12V	++++	++++
RacA G12V	+++	++++
RacB G12V	++++	++++
RacC G15V	++++	++++
RacD G17V	-	-
RacE G20V	-	-
RacF1 G12V	-	-
RacG G12V	-	-
RacH M13V	-	-
RacI S14V	-	-
RacJ D18V	-	-
RacL G12V	-	-
HsRac1 G12V	++++	++++
SpCdc42 GV12	++++	++++
HsRhoA G14V	-	-

Fig. 1. (A) WASP-B domain structure. (B) The genomic DNA was digested with *cla*I restriction enzyme and analyzed by Southern blotting with the *wasB* probe. (C) F-actin organization revealed by phalloidin staining in *wasB*$^-$ cells (bar = 5 μm). The bottom panel shows the ratio of intensity of F-actin staining at the foremost part (front) or rear end (back) of cells divided by the intensity at the center of the cells. The intensity value was acquired by line scan of images in the direction of the gradient (longitudinal) or perpendicular to the direction of the gradient (lateral) ($n = 10$). Error bars are SEM.*$p < 0.01$ versus A×3 (-cAMP), $^{\#}$ (+cAMP), Student's *t*-test. (D) Yeast two-hybrid analysis of interactions of the GBD of *Dictyostelium* WASP and WASP-B with constitutively active Rho GTPases found in *Dictyostelium* genome.

cells as little F-actin staining was detected at the lateral membrane. This polarity was partially maintained even in cells globally stimulated with cAMP. In contrast, *wasB*$^-$cells showed an increase in F-actin assembly throughout the lateral membrane, resulting in the less polarized F-actin organization even in the absence of cAMP stimulation.

3.2. Prolonged F-actin assembly following cAMP stimulation in wasB$^-$ cells

To examine the role of WASP-B in dynamic F-actin polymerization, *wasB*$^-$ cells were tested for *in vivo* actin polymerization responses to cAMP stimulation (Fig. 2A). Aggregation competent cells were lysed with lysis buffer at different time points following cAMP (1 μM) stimulation. Cytoskeletal fractions containing polymerized actin were collected by centrifugation at 18,000*g*, resolved on SDS–PAGE gels, and the intensity of the actin band was quantified. Wild type A×3 cells show a biphasic response to cAMP stimulation. The first phase occurs within 5–10 s after cAMP stimulation and consists of a significant increase of F-actin levels, followed by a decrease in actin levels. A second smaller peak of F-actin assembly is seen after about 40–60 s following cAMP stimulation. This second peak is associated with recruitment of plek-

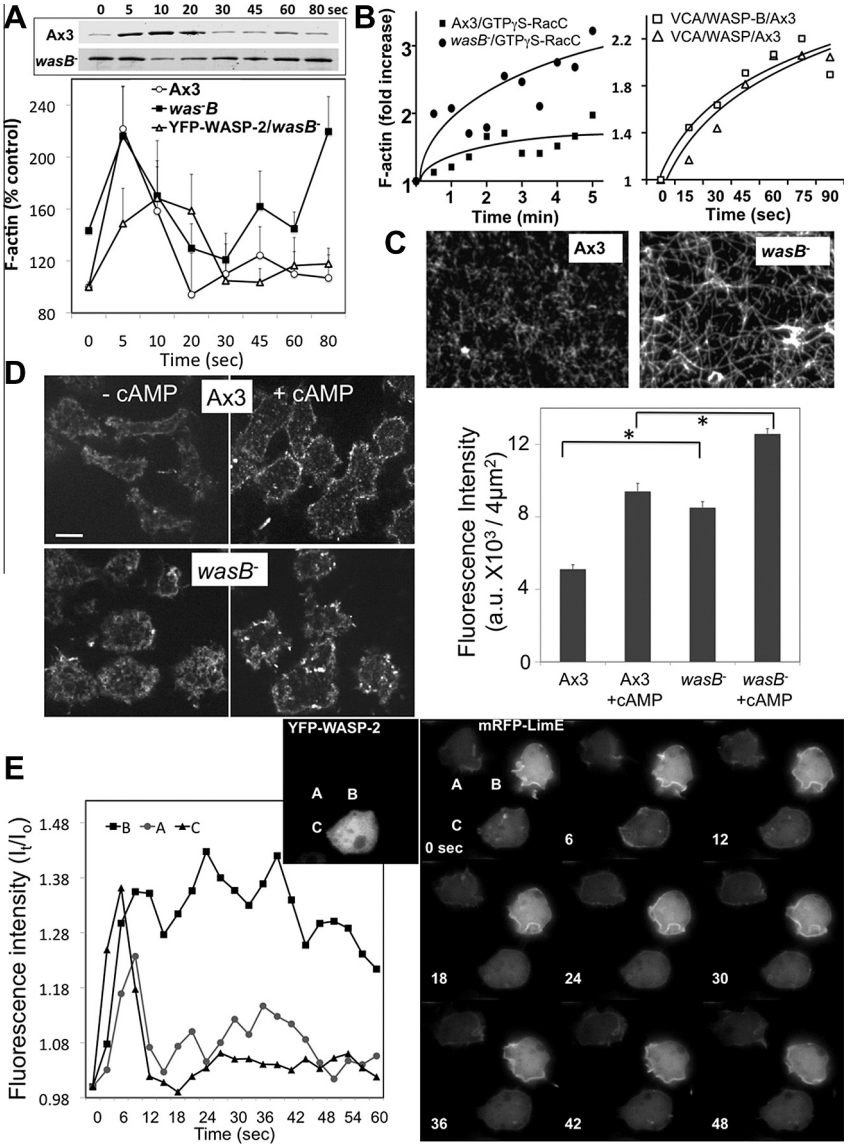

Fig. 2. Increased and prolonged F-actin polymerization response in *wasB*$^-$ cells. (A) *In vivo* actin polymerization assay measuring F-actin assembled in response to the cAMP stimulation. The top panel shows actin bands of the representative gel. Results were normalized to time 0 of wild type (A×3) cells. (B) *In vitro* F-actin polymerization assay. High-speed supernatants (HSS) were stimulated with GTPγS-bound RacC or VCA domains of WASP and WASP-B at time 0. Reactions were stopped at the indicated time points and F-actin was pelleted by centrifugation. Pellets were run on SDS–PAGE gels and the amount of F-actin at time 0 was standardized as 1. (C) Visualization of polymerized F-actin. HSS was incubated with or without 100 nM GTPγS-bound RacC for 1.5 min on a poly-D-lysine–treated glass coverslip and then fixed. (D) Labeling of actin nucleation sites (barbed ends). Stimulation of cells with cAMP was immediately followed by permeabilization and free barbed ends were stained with rhodamine-actin. The relative number of barbed ends (arbitrary units of fluorescence intensity) inside cells was measured ($n = 20$). Bar = 5 μm. $^*p < 0.01$. (E) F-actin organization revealed with mRFP-LimE-Δ-coil in live *wasB*$^-$ cells (cells A and B) or *wasB*$^-$ cells expressing YFP-WASP-B (cell C). Numbers in the lower left corner are seconds after stimulation. The right panel shows the translocation kinetics of mRFP-LimE-Δ-coil obtained from time-lapse recordings. The fluorescence intensity of membrane-localized mRFP fusion protein was quantified and compared to cytosolic intensity. The intensity ratio (I_t) between membrane and cytosol is plotted as a measure of the amount of membrane-associated protein relative to the starting conditions (I_0).

strin homology (PH) domain containing proteins to the membrane and can be disrupted by PI3K inhibition [16]. *wasB*$^-$ cells showed a higher basal level of F-actin than the wild type A×3 cells, which is consistent with the results of the phalloidin staining. *wasB*$^-$ cells appear to retain the first peak of F-actin polymerization upon cAMP stimulation. However, the main difference of *wasB*$^-$ cells from the wild type was that the size and duration of the second peak was much bigger and longer. The second peak of *wasB*$^-$ cells was as big as the first one and lasted over 20 s. Thus, the lack of *wasB* appears to have a positive impact on the size and duration of the F-actin assembly response upon cAMP stimulation. To support this data, *in vitro* F-actin polymerization assays were performed using high-speed supernatants (HSS) prepared from cAMP-pulsed *Dictyostelium* cells as described previously [17]. GTPγS-bound RacC initiated a roughly twofold stimulation of actin polymerization in the wild-type (A×3) supernatant, but stimulation of F-actin polymerization was much faster and greater in the *wasB*$^-$ supernatant (Fig. 2B). This result suggests that WASP-B might have an inhibitory role in the regulation of F-actin polymerization upon cAMP stimulation. It has been determined that the VCA domains of N-WASP, WASP, and Scar1 stimulate actin nucleation to different extents, with the N-WASP VCA region inducing nucleation 70-fold more quickly than Scar1 VCA domain [18]. Significantly lower Arp2/3-stimulating activity of WASP-B VCA domain might produce a level of stimulation low enough that would appear to be negatively contributing to actin polymeriza-

tion, especially when compared to the higher activity of WASP VCA domain for the Arp2/3 complex. We compared the activation potency of the VCA domains of WASP and WASP-B. Both GST–VCAs of WASP and WASP-B increased the rate of actin polymerization at similar levels (Fig. 2B). *In vitro* F-actin polymerization assays were repeated on glass coverslips and used to visualize assembled F-actin with fluorescent microscopy (Fig. 2C). Short actin filaments were observed in A×3 supernatant. In contrast, significantly elongated and branched filaments were found in *wasB*$^-$ supernatant. Actin assembly is regulated through the generation of free barbed ends. The number and location of free barbed ends that are available for F-actin polymerization was determined by labeling with rhodamine-actin in permeabilized cells (Fig. 2D). In aggregation-competent A×3 cells, the distribution of free barbed ends was localized to the periphery of cells and polarized toward the leading edge and uropod. Global cAMP stimulation caused equal distribution of free barbed ends around the periphery of cells, consistent with the change of cellular morphology, and some concentrated barbed ends were observed in the cell as bright spots. In contrast, the number of free barbed ends in *wasB*$^-$ cells was significantly greater than wild type cell, localizing not only around the periphery, but in the cell body too. Similarly to wild type cells, cAMP stimulation also caused appearance of bright puncta in the cell. These results indicate that the localization and number of free barbed ends are significantly altered in *wasB*$^-$ cells, suggesting that WASP-B is required for the proper regulation of F-actin polymerization. We examined the dynamic changes of the F-actin polymerization in live cells by observing the localization of a F-actin reporter, mRFP-LimE-Δ-coil [19] in *wasB*$^-$ cells (Fig. 2E). mRFP-LimE-Δ-coil fusion protein binds specifically and dynamically to F-actin. mRFP-LimE temporarily localized to the cortical membrane within 6 s after cAMP stimulation both in *wasB*$^-$ cells and *wasB*$^-$ cells expressing YFP-WASP-B. However, a clear difference was observed in later time in response to cAMP. mRFP intensity on the membrane drops back to basal level in *wasB*$^-$ cells expressing YFP-WASP-B after 30 s, but lasted significantly longer in *wasB*$^-$ cells, suggesting prolonged cortical F-actin polymerization. These results support the findings from our *in vivo* actin polymerization assay and suggest that WASP-B might play an inhibitory or, at least attenuating role in the regulation of F-actin polymerization.

3.3. Frequent protrusion of pseudopods causes aberrant chemotaxis of *wasB*$^-$ cells

To test whether the changes in the actin cytoskeleton described above alter chemoattractant-induced cell migration, images of chemotaxing cells were captured with time lapse microscopy and their movements were analyzed. The results show that wild type cells are well polarized and migrate quickly and linearly towards the chemoattractant source (Fig. 3; also see supplemental movies). We analyzed the motility of *Dictyostelium* cells with bimodal analysis, a method that compares time spent in persistent versus reorientation mode [20]. Bimodal analysis segregates the movements of a cell into alternating directional and reorientation modes based on the direction in which the cell is traveling. Bimodal analysis of the motility showed that wild type cells spent a relatively longer time in the directional mode than in the reorientation mode (Fig. 3A), thus migrating very directionally towards the cAMP source. *wasB*$^-$ cells did not migrate efficiently towards the cAMP source even though they were polarized and could sense the chemoattractant source as, over time, they migrate towards the source. *wasB*$^-$ cells changed their directions quite often, resulting in spending a significantly longer time in the reorientation mode rather than making directional displacements. This is consistent with a lower chemotaxis index and a decreased velocity of *wasB*$^-$ cells when compared to that of wild type cells (Fig. 3B). Expression of YFP-WASP-B in *wasB*$^-$ cells appears to rescue this defect as the cells move quite directionally, resulting in a higher chemotaxis index and greater velocity. To examine chemotaxis defects of *wasB*$^-$ cells more closely, we measured the number and lifespan of pseudopods extended from the wild type and *wasB*$^-$ cells (Fig. 3C and D). Wild type cells generally extend pseudopodia in the direction of the chemoattractant, creating few lateral and rear pseudopodia. *wasB*$^-$ cells extend rear and lateral pseudopods almost twice as frequent as wild type cells. Moreover, the average lifespan of pseudopods in *wasB*$^-$ cells was ~75% longer than in wild type cells. This contributed to the inefficient chemotaxis of *wasB*$^-$ cells. Recent studies [21] found that nearly all pseudopodia produced during chemotaxis fall into one of two categories: (1) those that form by splitting from existing pseudopodia (split pseudopodia), or (2) those that are produced at apparently random positions around the cell cortex (*de novo* pseudopodia). *wasB*$^-$ cells (*de novo*: split ratio = 3.6) clearly showed more *de novo* pseudopodia than wild type cells (*de novo*: split ratio = 0.14). Expression of YFP-WASP-B restored the ratio back to a level similar to that of the wild type cells. These results indicate that the extension of rear and lateral *de novo* pseudopods disrupts the directional movement of these cells in a particular direction.

3.4. Subcellular localization of YFP-WASP-B

In an attempt to examine spatio-temporal localization of WASP-B, we examined *wasB*$^-$ cells expressing YFP-WASP-B. Phalloidin staining of these cells revealed almost uniform distribution of YFP-WASP-B at a steady state and absence of YFP-WASP-B at newly formed pseudopods where F-actin is enriched (Fig. 4A). Examination of YFP-WASP-B localization in live cells reveals lack of specific localization of YFP-WASP-B. There might be a temporary absence of YFP-WASP-B localization in developing pseupods especially at an early stage. (Fig. 4B). Many proteins involved in F-actin polymerization such as WIPa [14] translocates to the cell cortex upon global cAMP stimulation. However, examination of YFP-WASP-B localization upon cAMP stimulation exhibited no translocation to cortical membrane (not shown). This result was confirmed by determining the association of YFP-WASP-B with the detergent insoluble cytoskeleton/membrane fraction (DIF) (Fig. 4D). Aggregation competent *wasB*$^-$ cells expressing YFP-WASP-B were stimulated with 1 μM cAMP and lysed with lysis buffer. DIF was pelleted by spinning lysate at 18,000 rpm. The association of YFP-WASP-B with the DIF was detected by western blot. Upon cAMP stimulation, Most YFP-WASP-B remain in the detergent-soluble fraction as little amount of YFP-WASP-B translocates into the detergent-insoluble cytoskeleton fraction. These results indicate that the localization of WASP-B do not change upon cAMP stimulation. WASP is thought to be localized to the anterior leading edge of chemotaxing cells by binding of the basic domain to phosphoinositides ($PI(4,5)P_2$ or $PI(3,4,5)P_3$) on the anterior membrane [3,4,10]. In contrast, WASP-B does not have an obvious stretch of basic residues. Thus, WASP-B might have less strict control on its localization. We demonstrated that WASP-B appears to be rather uniformly distributed in the cytoplasm either at steady state or in live cells and, surprisingly, not in protruding pseupodia where WASP localizes [10], indicating that WASP-B localization does not overlap with F-actin polymerization. This also suggests a negative regulatory role of WASP-B in controlling F-actin polymerization.

3.5. Aberrant regulation of RacC in *wasB*$^-$ cells

Our previous study examined the interactions between the GBD domains of WASP with specific Rho GTPases [22]. Through the use of a yeast two-hybrid analysis, we found that WASP and WASP-B showed exactly the same binding preference to RacC, RacB, and

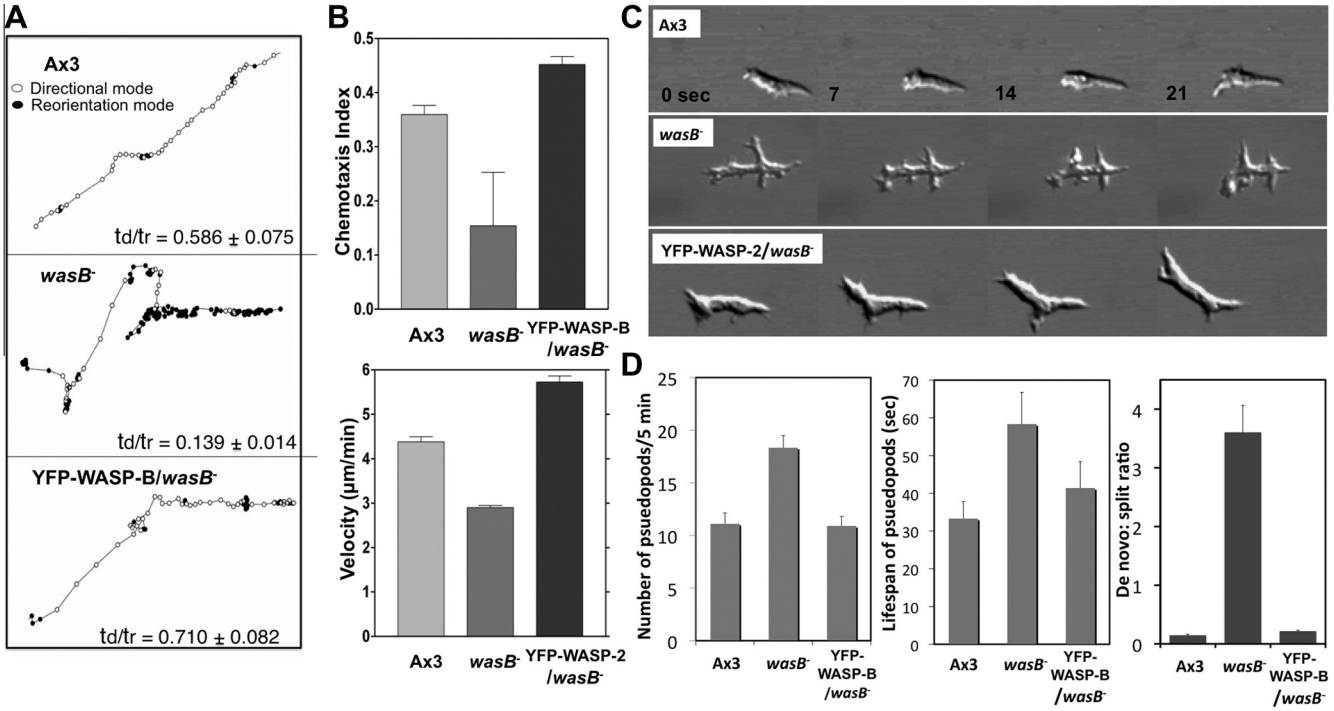

Fig. 3. Defects in chemotaxis of *wasB*⁻ cells. (A) Bimodal analysis of chemotactic movement of wild type, *wasB*⁻, or *wasB*⁻ cells expressing YFP-WASP-B with a 5 s sampling interval over 15 min is shown. (B) Chemotaxis indices indicate that *wasB*⁻ cells showed inefficient chemotaxis toward micropipette. *wasB*⁻ cells expressing YFP-WASP-B migrate as efficiently as wild type cells, showing a rescue of the phenotype. (C) Loss of WASP-B function decreases the velocity with which cells chemotax. *wasB*⁻ cells expressing YFP-WASP-B migrate as rapidly as wild type cells. (D) Montage of cells migrating towards the chemoattractant source. (E) Number of pseupods made by a single cell over 5 min periods. *wasB*⁻ cells make twice as many pseupods as A×3 cells. Lifespan of pseudopods made by *wasB*⁻ cells is twice as long as A×3 cells. Ratio between *de novo* and split pseudopodia is significantly higher in *wasB*⁻ cells than in A×3 cells.

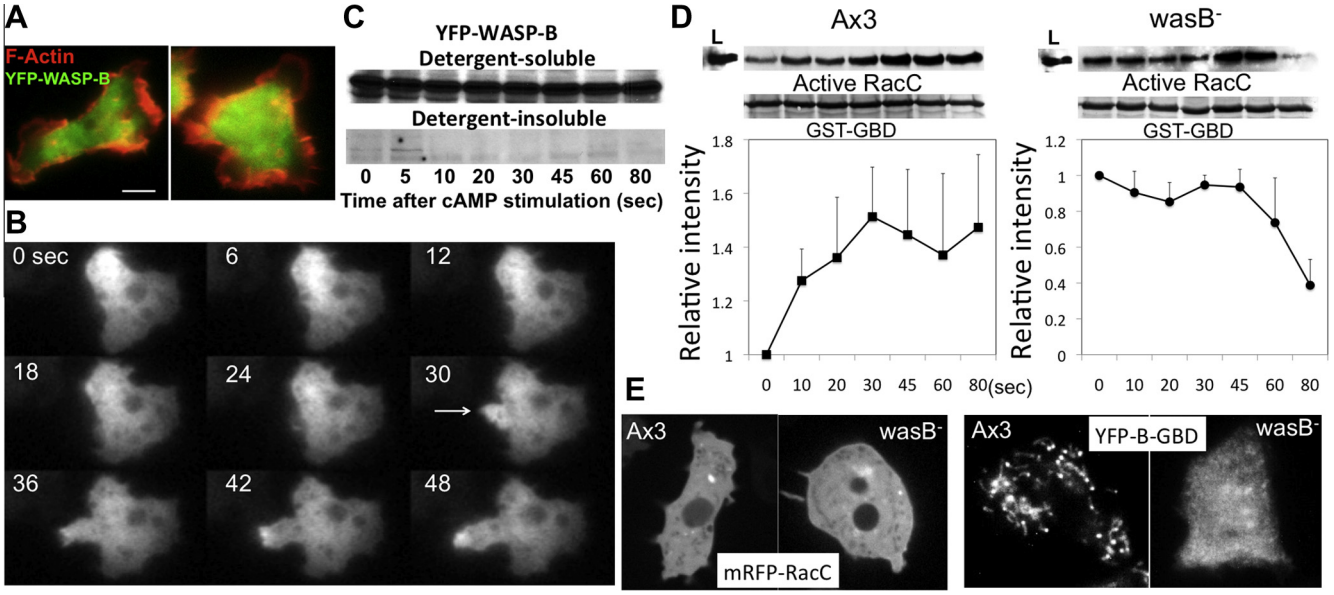

Fig. 4. (A) Aggregation-competent *wasB*⁻ cells expressing YFP-WASP-B were fixed and stained with Texas-red-labeled phalloidin and representative image is shown. Bar = 5 μm. (B) Localization of YFP-WASP-B in live cells. Aggregation-competent *wasB*⁻ cells expressing YFP-WASP-B were imaged at every 3 s. Arrow indicates protruding pseupods. (C) *wasB*⁻ cells expressing YFP-WASP-B were stimulated with 1 μM cAMP and lysates were collected at indicated times and detergent-insoluble cytoskeletal fractions were obtained by centrifugation. YFP-WASP-B was detected by western blotting with GFP antibody. (D) Time course pull-downs of active RacC with GST-GBD were performed in a different time points after cAMP stimulation. The top Western blot shows the level of active RacC isolated by pulldown assay and the total amount of RacC in the lysate (L); the lower blot shows the total amount of GST-GBD used for pull-down. Intensities of bands were measured and average of three blots were plotted graphically for A×3 and *wasB*⁻ cells. (E) Localization of mRFP-RacC and YFP-B-GBD in live A×3 and *wasB*⁻ cells.

Rac1B (Fig. 1D), suggesting a possibility that WASP and WASP-B might compete for the binding of active Rho GTPases. Thus, it is plausible that more active RacC might be available for downstream effectors in *wasB*⁻ cells. To directly test this hypothesis, we used an affinity precipitation assay, which takes advantage of the selective interaction of the GBD domain of WASP with active RacC[GTP].

A×3 and *wasB*$^-$ cells expressing CFP-RacC were lysed at 0, 10, 20, 30, 45, 60, and 80-s after cAMP stimulation and active CFP-RacC was pulled down with GST-GBD beads and relative amount of active RacC in different time points was determined by western blots as shown in Fig. 4D. A clear difference in the basal level of active RacC was observed as ~60% of total RacC in lysate can be pulled down with GST-GBD in *wasB*$^-$ cells compared to ~35% in A×3 cells, indicating higher level of active RacC in *wasB*$^-$ cells. This result suggests that RacC is not competing for binding between the two GBD domains in *wasB*$^-$ cells and that more active RacC is present in *wasB*$^-$ cells, which might drive more F-actin polymerization as manifested in our earlier assays. Kinetics of RacC activation also showed a clear difference. The level of active RacC gradually increased and peaked at 30–45 s after cAMP stimulation in A×3 cells, but stayed at a constant level until 45 s and rapidly decreased in *wasB*$^-$ cells. mRFP-RacC in live A×3 and *wasB*$^-$ cells was uniformly distributed in the cytoplasm (Fig. 4E). YFP-B-GBD (a reporter for active RacC) was localized to vesicular structures concentrated in the front of A×3 cells as we described in our previous study [10]. However, YFP-B-GBD is rather uniformly distributed in *wasB*$^-$ cells, suggesting aberrant localization of active RacC in *wasB*$^-$ cells. Thus, chemotaxis defects of *wasB*$^-$ cells are likely to result from the aberrant regulation of RacC activation and localization.

Acknowledgments

We thank Drs. Alissa Weaver and Scott Gruver for invaluable technical assistance and useful discussions. This work was supported, in part, by a grant from National Institute of Health (GM68097 to C.Y.C.).

References

[1] T.H. Millard, S.J. Sharp, L.M. Machesky, Signalling to actin assembly via the WASP (Wiskott–Aldrich syndrome protein)- family proteins and the Arp2/3 complex, Biochem. J. 380 (2004) 1–16.
[2] S.H. Zigmond, How WASP regulated actin polymerization, J. Cell Biol. 150 (2000) F117–F120.
[3] K.E. Prehoda, J.A. Scott, R.D. Mullins, W.A. Lim, Integration of multiple signals through cooperative regulation of the N-WASP-Arp2/3 complex, Science 290 (2000) 801–806.
[4] H.N. Higgs, T.D. Pollard, Activation by Cdc42 and PIP(2) of Wiskott–Aldrich syndrome protein (WASp) stimulates actin nucleation by Arp2/3 complex, J. Cell Biol. 150 (2000) 1311–1320.
[5] L.M. Machesky, R.H. Insall, R.R. Kay, The helC gene encodes a putative DEAD-box RNA helicase required for development in *Dictyostelium discoideum*, Curr. Biol. 8 (1998) 607–610.
[6] M. Tsujioka, L.M. Machesky, S.L. Cole, K. Yahata, K. Inouye, A unique talin homologue with a villin headpiece-like domain is required for multicellular morphogenesis in *Dictyostelium*, Curr. Biol. 9 (1999) 389–392.
[7] R.D. Mullins, T.D. Pollard, Structure and function of the Arp2/3 complex, Curr. Opin. Struct. Biol. 9 (1999) 244–249.
[8] T.M. Svitkina, A.B. Verkhovsky, K.M. McQuade, G.G. Borisy, Analysis of the actin-myosin II system in fish epidermal keratocytes: mechanism of cell body translocation, J. Cell Biol. 139 (1997) 397–415.
[9] D. Pantaloni, R. Boujemaa, D. Didry, P. Gounon, M.F. Carlier, The Arp2/3 complex branches filament barbed ends: functional antagonism with capping proteins, Nat. Cell Biol. 2 (2000) 385–391.
[10] S. Myers, J.W. Han, Y. Lee, R. Firtel, C.Y. Chung, A *Dictyostelium* homologue of WASP is required for polarized F-actin assembly during chemotaxis, Mol. Biol. Cell 16 (2005) 2191–2206.
[11] P. Fey, P. Gaudet, T. Curk, B. Zupan, E.M. Just, S. Basu, S.N. Merchant, Y.A. Bushmanova, G. Shaulsky, W.A. Kibbe, R.L. Chisholm, Dictybase–a *Dictyostelium* bioinformatics resource update, Nucl. Acids Res. 37 (2009) D515–D519.
[12] G. Vlahou, F. Rivero, Rho GTPase signaling in *Dictyostelium discoideum*: insights from the genome, Eur. J. Cell Biol. 85 (2006) 947–959.
[13] M. de la Roche, A. Mahasneh, S.-F. Lee, F. Rivero, G.P. Cote, Cellular distribution and functions of wild-type and constitutively activated *Dictyostelium* PakB, Mol. Biol. Cell 16 (2005) 238–247.
[14] S.A. Myers, L.R. Leeper, C.Y. Chung, WASP-interacting protein (WIPa) is important for actin filament elongation and prompt pseudopod formation in response to a dynamic chemoattractant gradient, Mol. Biol. Cell 17 (2006) 4564–4575.
[15] R.A. Firtel, C.Y. Chung, The molecular genetics of chemotaxis: sensing and responding to chemoattractant gradients, Bioessays 22 (2000) 603–615.
[16] L. Chen, C. Janetopoulous, Y.E. Huang, M. Iijima, J. Borleis, P.N. Devroeotes, Two phases of actin polymerization display different dependencies on PI(3,4,5)P_3 accumulation and have unique roles during chemotaxis, Mol. Biol. Cell 14 (2003) 5028–5037.
[17] S.H. Zigmond, M. Joyce, J. Borleis, G.M. Bokoch, P.N. Devreotes, Regulation of actin polymerization in cell-free systems by GTPgammaS and Cdc42, J. Cell Biol. 138 (1997) 363–374.
[18] J. Zalevsky, L. Lempert, H. Kranitz, R.D. Mullins, Different WASP family proteins stimulate different ARP2/3 complex-dependent actin- nucleating activities, Curr. Biol. 11 (2001) 1903–1913.
[19] T. Bretschneider, S. Diez, K. Anderson, J. Heuser, M. Clarke, A. Muller-Taubenberger, J. Kohler, G. Gerisch, Dynamic actin patterns and Arp2/3 assembly at the substrate- attached surface of motile cells, Curr. Biol. 14 (2004) 1–10.
[20] J.S. Gruver, A.A. Potdar, J. Jeon, J. Sai, B. Anderson, D. Webb, A. Richmond, V. Quaranta, P.T. Cummings, C.Y. Chung, Bimodal analysis reveals a general scaling law governing nondirected and chemotactic cell motility, Biophys. J. 99 (2010) 367–376.
[21] L. Bosgraaf, P.J. Van Haastert, The ordered extension of pseudopodia by amoeboid cells in the absence of external cues, PLoS One 4 (2009) e5253.
[22] J.W. Han, L. Leeper, F. Rivero, C.Y. Chung, Role of RacC for the regulation of wasp and phosphatidylinositol 3-kinase during chemotaxis of *Dictyostelium*, J. Biol. Chem. 281 (2006) 35224–35234.